Rapid Communications

Coulomb-induced instabilities of nodal surfaces

Pavel A. Volkov[1,2] and Sergej Moroz[3]

[1]*Theoretische Physik III, Ruhr-Universität Bochum, D-44780 Bochum, Germany*

[2]*Department of Physics and Astronomy, Center for Materials Theory, Rutgers University, Piscataway, New Jersey 08854, USA*

[3]*Department of Physics, Technical University of Munich, D-85748 Garching, Germany*

(Received 30 July 2018; published 13 December 2018)

We consider the stability of nodal surfaces in fermionic band systems with respect to the Coulomb repulsion. It is shown that nodal surfaces at the Fermi level are gapped out at low temperatures due to emergent particle-hole orders. Energy dispersion of the nodal surface suppresses the instability through an inhomogeneous phase. We argue that around criticality the order parameter fluctuations can induce superconductivity. We show that by tuning doping and disorder one could access various phases, establishing fermionic nodal surface systems as a versatile platform to study emergent quantum orders.

DOI: 10.1103/PhysRevB.98.241107

Introduction. The last decade saw a surge of research activity aimed at a better understanding of the physics of nodal objects in three-dimensional (3D) fermionic band structures [1–3]. Most studied is the case of Weyl semimetals with nodal points, recently discovered experimentally [4,5]. They generically appear in any band structure provided time-reversal or inversion symmetry is broken. Remarkably, nodal points do not exhaust all possible nodal objects in a three-dimensional band structure. In 2011, Weyl nodal loops, where two bands intersect each other on closed two-dimensional (2D) curves, were predicted [6–8]. A generic nodal loop has to be protected by symmetries. It is distinguished by a π Berry phase on a contour that links with it and exhibits nearly flat drumhead states in the boundary spectrum [8,9].

More recently, another type of nodal object was proposed—a nodal surface [10,11]. The nodal surface is a two-dimensional degeneracy of energy bands that forms a closed surface in the Brillouin zone. While less generic then the nodal points, they can nevertheless appear in systems that possess certain additional symmetries, such as sublattice or mirror symmetries. Nodal surfaces protected by different symmetries were theoretically predicted [12–17] and their topological stability against small perturbations of the noninteracting Bloch Hamiltonian was investigated [14–16]. Material realizations of nodal surfaces were also proposed [17,18].

However, to understand the robustness of nodal objects in real solids it is imperative to study their stability with respect to interactions. In Weyl point [19–21] and loop [22] semimetals it has been shown that short-range interactions need to be stronger than a certain threshold to destroy the nodal structures. The long-range part of the Coulomb interaction is marginally irrelevant [23,24] in the case of Weyl points. In nodal line systems the Coulomb interaction is partially screened, but turns out to be irrelevant as well [25]. On the other hand, introducing a finite density of states by breaking inversion symmetry [26] or doping [27,28] results in instabilities already at weak coupling.

In this Rapid Communication, we study the fate of nodal surfaces in the presence of the Coulomb interaction. First, we show that the long-range part of the Coulomb interaction renders nodal surfaces at the Fermi level unstable to the formation of an "excitonic insulator," first proposed by Keldysh and Kopaev in the seminal paper [29]. Subsequently, we demonstrate that the energy dispersion of the nodal surface suppresses the instability. We specify our discussion to the case where the band structure has twofold degeneracy in the Brillouin zone supplemented by spin rotational invariance, giving rise to the so-called Dirac nodal surface. We analyze the emerging orders in the mean-field approximation for different combinations of short- and long-range repulsion and in the presence of sublattice symmetry. Additionally, we show that doping and disorder can serve as experimental "knobs" that grant access to various phases including the particle-hole counterpart of the elusive Fulde-Ferrell-Larkin-Ovchinnikov (FFLO) state [30,31] of superconductors. Finally, we argue that fluctuations of the particle-hole order parameter might lead to unconventional superconductivity in the vicinity of the doping-induced quantum critical point (QCP).

Particle-hole instability of the nodal surface. We start by showing that long-range Coulomb repulsion can render nodal surfaces unstable. First, we consider the case of a particle-hole symmetric Weyl nodal surface at the Fermi energy described by the two-band Hamiltonian

$$\hat{H}_0 = \sum_{\mathbf{p}} \hat{c}^\dagger_{\mathbf{p}} \varepsilon(\mathbf{p}) \sigma_z \hat{c}_{\mathbf{p}}, \tag{1}$$

where the energy $\varepsilon(\mathbf{p})$ is measured with respect to the Fermi level. In what follows, we will use the linearized form of the dispersion near the Fermi level $\varepsilon(\mathbf{p}) \approx \mathbf{v}_F(\theta,\varphi) \cdot [\mathbf{p} - \mathbf{p}_F(\theta,\varphi)]$, where θ and φ are the angles in spherical coordinates, assuming $|\mathbf{v}_F(\theta,\varphi)| \neq 0$. Without an interaction, the system described by (1) contains an electron- and a holelike Fermi surface that coincide in the momentum space [see Fig. 1(a)]. For the following discussion we will consider the generalization of (1) to the case with N_0 identical nodal surfaces, which results in N_0 pairs of coinciding electron- and holelike Fermi surfaces.

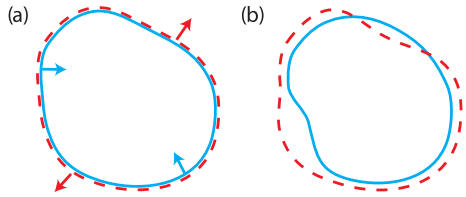

FIG. 1. Two-dimensional projection of the electron (dashed red) and hole (solid blue) Fermi surfaces for a system with a nodal surface (1) (a) at zero energy; arrows show the direction of Fermi velocities (b) with energy dispersion (see text); crossings of the two surfaces are projections of a single zero-energy nodal line.

Importantly, the system has a finite density of itinerant charge carriers and the Coulomb potential is screened. In the random phase approximation (that can be justified in the regime $N_0 \gg 1$ [32,33]) one has $4\pi e^2/\mathbf{q}^2 \to [\mathbf{q}^2/4\pi e^2 - \Pi(i\omega_n, \mathbf{q})]^{-1}$. To study the low-energy effects we approximate the interaction by its static ($\omega_n = 0$) value at low momenta [34] such that $\Pi(i\omega_n, \mathbf{q})$ reduces to $-\nu$ (ν being the total density of states) resulting in

$$\hat{H}_{\rm Coul} \approx \frac{U_0}{2\mathcal{V}} \sum_{\mathbf{p},\mathbf{p}',\mathbf{q}} \hat{c}^\dagger_{\mathbf{p}+\mathbf{q},\sigma} \hat{c}^\dagger_{\mathbf{p}'-\mathbf{q},\sigma'} \hat{c}_{\mathbf{p}',\sigma'} \hat{c}_{\mathbf{p},\sigma}, \tag{2}$$

where $\mathcal{V}$ is the volume of the system and $U_0 = \nu^{-1}$. Note that $\nu = 2N_0\nu_0$, where ν_0 is the density of states of a single Fermi surface (electron- or holelike).

Let us now consider the possible instabilities of (1) with interaction (2). Decoupling the repulsive interaction (2) with the Hubbard-Stratonovich procedure, one immediately finds that the particle-hole channels with order parameters $W_i(\mathbf{Q}) = U_0 \sum_{\mathbf{p}} \langle \hat{c}^\dagger_{\mathbf{p}} \sigma_i \hat{c}_{\mathbf{p}+\mathbf{Q}} \rangle$ are all attractive with the same coupling constant. Moreover, the W_x and W_y orders for $\mathbf{Q} = \mathbf{0}$ can be shown to develop a weak-coupling instability. The self-consistency equation for these orders has the form

$$\frac{1}{U_0} = \frac{\nu_0}{2} \int d\varepsilon \frac{\tanh \frac{\sqrt{\varepsilon^2+W^2}}{2T}}{\sqrt{\varepsilon^2+W^2}}, \tag{3}$$

where the density of states is approximated by a constant $\nu(\varepsilon) \approx \nu_0$ and $W = \sqrt{W_x^2 + W_y^2}$. Due to the logarithmic divergence of the right-hand side at low temperatures we see that a transition occurs for an arbitrary weak coupling with the critical temperature being

$$T_c = \frac{2e^\gamma}{\pi} \Lambda e^{-2N_0}, \tag{4}$$

and the value of the order parameter at zero temperature $W_0 = 2\Lambda e^{-2N_0}$, where Λ is the upper cutoff for the energy integral in Eq. (3). Physically, Λ is determined by the structure of the dispersion in (1) away from the Fermi surface. In particular, it is fixed by the bandwidth and the Fermi energy with respect to the band bottom. The eigenenergies in the presence of the order parameter are $E(\mathbf{p}) = \pm\sqrt{\varepsilon(\mathbf{p})^2 + W^2}$, clearly showing that a gap has opened and the nodal surface is destroyed.

For a single Weyl nodal surface ($N_0 = 1$), the transition corresponds to breaking of a global $U(1)_z$ symmetry generated by $\sum_{\mathbf{p}} \hat{c}^\dagger_{\mathbf{p}} \sigma_z \hat{c}_{\mathbf{p}}$. We note that the degeneracy between W_x and W_y orders is due to the highly symmetric form of the interaction (2); additional interactions can break this degeneracy such that only a particular linear combination of them will develop a nonzero expectation value. However, if these additional interactions are much smaller than U_0, the equations for T_c and W_0 will approximately hold. We discuss in detail the influence of additional interactions below for the case of a Dirac nodal surface.

Nodal surfaces with energy dispersion. While the presence of nodal surfaces in the band structure can be guaranteed by symmetry and the ensuing topological invariants [14], they do not have to be pinned to the Fermi energy. Indeed, a term of the form $f(\mathbf{p})\sigma_0$ can be always added to the Hamiltonian (1) without breaking any symmetries generated by σ_i. This term shifts the nodal surface $\varepsilon(\mathbf{p}) = 0$ to an energy $f(\mathbf{p})$ and breaks the particle-hole symmetry. As a result, a generic nodal surface coincides with Fermi surfaces on a set of loops in momentum space.

Physically, a constant $f(\mathbf{p}) = f_0$ is equivalent to a shift of the chemical potential. Consequently, a constant f_0 can be experimentally realized by doping electrons/holes into the system. The momentum dependence of $f(\mathbf{p})$, on the other hand, is determined by the specific material. For the particular case of a Dirac nodal surface protected by sublattice symmetry (see below), $f(\mathbf{p})$ corresponds to intrasublattice hopping.

We can now expand the function $f(\mathbf{p})$ near the Fermi surface $f(\mathbf{p}) \approx \gamma(\theta,\varphi) + \delta(\theta,\varphi)\varepsilon(\mathbf{p}) + O(\varepsilon^2)$. The resulting eigenenergies of the free Hamiltonian are then $E_\pm = [\delta(\theta,\varphi) \pm 1]\varepsilon(\mathbf{p}) + \gamma(\theta,\varphi)$. $\gamma(\theta,\varphi)$ leads to the electron and hole Fermi surfaces no longer being coincident [see Fig. 1(b)], while $\delta(\theta,\varphi)$ gives rise to a difference between the Fermi velocities of the electron and hole bands. The latter can be shown [35] not to destroy the weak-coupling instability.

Let us now analyze the physical consequences of a constant $\gamma(\theta,\varphi) = \gamma_0$. We assume $\gamma_0 \ll E_F$ such that the density of states remains unchanged. In this case the mean-field Hamiltonian can be written as

$$H_{\rm MF} = \begin{bmatrix} \hat{c}_{\mathbf{p},1} \\ \hat{c}_{\mathbf{p},2} \end{bmatrix}^\dagger \begin{bmatrix} \varepsilon(\mathbf{p}) + \gamma_0 & W_x - iW_y \\ W_x + iW_y & -\varepsilon(\mathbf{p}) + \gamma_0 \end{bmatrix} \begin{bmatrix} \hat{c}_{\mathbf{p},1} \\ \hat{c}_{\mathbf{p},2} \end{bmatrix}.$$

One can note the similarity to the Hamiltonian of a superconductor in a Zeeman field. As is well known [31], at low temperature the order parameter vanishes via a first-order transition at the Clogston-Chandrasekar limit $\gamma_0^{\rm cr} = W_0/\sqrt{2}$, where W_0 is the order parameter in the absence of the Zeeman field. This implies that γ_0 stabilizes the nodal surface against weak enough interactions.

Importantly, the first-order phase transition is preempted by an instability to the formation of a periodically modulated state [30,31,36]. In our case this corresponds to a particle-hole order parameter of the form $\hat{c}^\dagger_{\alpha,\mathbf{p}+\mathbf{Q}} \hat{c}_{\alpha',\mathbf{p}}$, i.e., a charge, spin, or bond current density wave. A formal analogy extends also to itinerant antiferromagnets [37–39]. A qualitative phase diagram is presented in Fig. 2. As the details of the modulated (incommensurate) phase such as the direction and magnitude of the modulation wave vector are quite sensitive to the Fermi-surface details, we do not consider them here. Generally, one would expect $\mathbf{Q}$ to connect the points with opposite Fermi velocities with the lowest curvature. Hence,

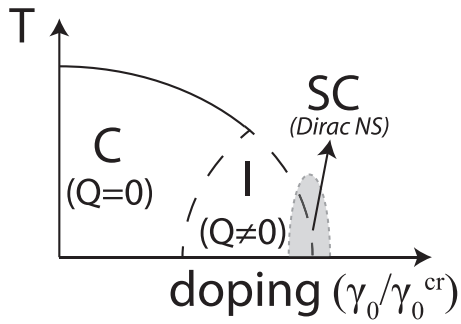

FIG. 2. Tentative temperature-doping phase diagram for a nodal surface system with repulsive interaction. The doping scale is given by the value of γ_0 (see text) normalized to $\gamma_0^{cr} = W_0/\sqrt{2}$. "C" is the commensurate (homogeneous) particle-hole order, while "I" is the modulated phase. A superconducting (SC) phase around the particle-hole QCP (shaded gray area) could emerge for the Dirac nodal surfaces.

low dimensionality and the presence of flat portions of the Fermi surface promote such phases [36].

Let us move on to the effect of a nonconstant $\gamma(\theta,\varphi)$. For the homogenous order, given the critical temperature T_c for $\gamma = 0$ (4), one can extract the new critical temperature T_c' from the equation [35] $\log\frac{T_c'}{T_c} = -\frac{1}{2}\langle\psi(\frac{1}{2}+\frac{i|\gamma|}{2\pi T_c'}) + \psi(\frac{1}{2}-\frac{i|\gamma|}{2\pi T_c'}) - 2\psi(\frac{1}{2})\rangle_{\rm FS}$, where $\psi(z)$ is the digamma function and $\langle\cdots\rangle_{\rm FS} = \int\cdots\frac{\nu_0(\varepsilon=0,\theta,\varphi)d\Omega}{4\pi\nu_0}$. We observe that the physical effect of T_c suppression is present even if $\langle\gamma\rangle_{\rm FS} = 0$. At low temperatures, unlike for $\gamma = $ const, the order parameter may change its value before disappearing, since electron/hole pockets can start to appear in regions where $|\gamma(\theta,\varphi)| > W_0$. We note that for the incommensurate phases the results will depend on the particular realization of $\gamma(\mathbf{p})$ and thus we shall not consider them here.

Dirac nodal surface. Up to now, we have not discussed the physical meaning of the emergent orders W_i. To do so, we need to know how the fermionic operators $\hat{c}_\mathbf{p}$ change under symmetry operations, which, in general, depends on the system. Here, we analyze the particular case of a single Dirac nodal surface ($N_0 = 2$) protected by inversion-enriched time-reversal symmetry (TRS+I) and sublattice symmetry on a bipartite lattice (BDI class in Ref. [14]). In this case the system has full spin rotational invariance and the Hamiltonian retains the form (1), being trivial (unity matrix) in spin space. On the other hand, in the sublattice basis the Hamiltonian has to be off-diagonal due to the sublattice symmetry. Moreover, the inversion-enriched TRS acts as a complex conjugation (but does not flip the momentum) leading to $H(\mathbf{p}) = H^*(\mathbf{p})$. Consequently, the tight-binding Hamiltonian respecting the symmetry can contain only the real intersublattice hopping $\sim\sigma_x$. Thus the unitary transformation $U = (\sigma_x+\sigma_z)/\sqrt{2}$, which acts as $U^{-1}\sigma_z U = \sigma_x$, transforms the operators from the "band basis" of (1) to the sublattice basis.

The instability analysis performed above can be directly applied to the Dirac nodal surface problem. However, apart from W_x and W_y, spinful orders $W_{i,j} = U_0\sum_\mathbf{p}\langle\hat{c}_\mathbf{p}^\dagger\sigma_i s_j\hat{c}_\mathbf{p}\rangle$, where $i = x, y$ and s_j denotes the set of spin Pauli matrices, also develop weak-coupling instabilities.

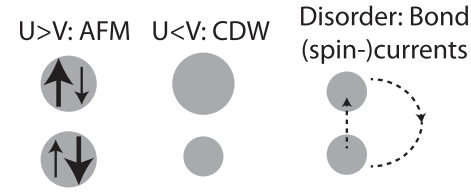

FIG. 3. An illustration of the emergent states possible for a single Dirac nodal surface. Above the illustrations the necessary conditions for their realization are given.

Now let us identify the physical meaning of the respective orders. Since $\sigma_x \xrightarrow{U} \sigma_z$, the W_x order parameter has the meaning of an energy offset between the two sublattices. This leads in turn to a charge offset resulting in a charge density wave (CDW). Note that the CDW in this case breaks only the sublattice, but not translational symmetry. $\sigma_y \xrightarrow{U} -\sigma_y$ and thus in the sublattice basis the W_y order introduces a nonzero average $i\langle\hat{c}_A^\dagger\hat{c}_B - \hat{c}_B^\dagger\hat{c}_A\rangle$ that implies a current flowing between different sublattice sites A and B. Since in the ground state the total current between the sublattices should be zero, compensating interunit cell currents should be also present with their structure being determined by the form of $\varepsilon(\mathbf{p})$. The CDW/bond current orders, discussed above, preserve/break TRS, respectively. Turning now to spin orders, one observes that $W_{x,i}$ break both sublattice and time-reversal symmetry and essentially represent intraunit cell antiferromagnetism (AFM). On the other hand, the orders $W_{y,i}$ do not break TRS and correspond to spin current order.

The interaction (2) results in the orders $W_{x,i}$ and $W_{y,i}$ forming a degenerate manifold. However, as the represented orders break different symmetries, one would expect this degeneracy to be accidental. Indeed, we show now that the inclusion of the simplest on-site interactions allowed by symmetry lifts this degeneracy. Namely, let us add the on-site Hubbard repulsion $U[\hat{n}_\uparrow^A\hat{n}_\downarrow^A + \hat{n}_\uparrow^B\hat{n}_\downarrow^B]$ and the repulsion between the two sublattices $V\hat{n}^A\hat{n}^B$, where we introduced the densities $\hat{n}^{A(B)} = \hat{c}^\dagger(1\pm\sigma_x)\hat{c}/2$. Decoupling these interactions [35] with respect to the same channels as before, we get corrections to the transition temperatures (4) resulting from $2N_0 \to [1/(2N_0) - \mathcal{V}_0\nu_0\lambda_{i,j}]^{-1}$, where $\mathcal{V}_0$ is the unit cell volume. The coupling constants for the orders $W_{i,j}$ are $\lambda_{x,0} = U - 2V$, $\lambda_{x,\{x,y,z\}} = -U$, and $\lambda_{y,\{0,x,y,z\}} = -V$. Consequently, for $U > V$, the intraunit cell antiferromagnetic order is the leading one, while for $U < V$ the CDW order wins (see Fig. 3). Note that the influence of the short-range interactions can be controlled by the density of states ν_0, i.e., for dilute systems the screened Coulomb interaction (2) is still the dominant one. On the other hand, we consider $\lambda_{i,j}$ to be not too small, such that the fluctuations of competing orders could be neglected.

Effects of disorder. As nodal surface systems are 3D metals with a finite density of states, weak disorder that preserves all symmetries is not expected to disrupt the nodal surfaces [40,41]. On the other hand, interaction-induced particle-hole orders can be suppressed even for low-impurity concentrations. We show below that this effect allows one to promote the (otherwise subleading) staggered current phase discussed above (see Fig. 3).

We perform the calculation in the framework of Abrikosov-Gor'kov theory [42]. Namely, let us consider the impurity potential affecting atoms of one of the sublattices only, corresponding to a single-site substitution or vacancy, with the Hamiltonian $\hat{H}_{\rm imp} = u/\sqrt{2}\hat{c}^\dagger(\mathbf{r}_0)(1 \pm \sigma_x) \otimes s_0\hat{c}(\mathbf{r}_0)$ (for other types of impurities, see Ref. [35]). Assuming randomly distributed impurity positions, one obtains the equation for the critical temperature T_c^d in the presence of disorder for the case of weak dilute impurities ($up_F^3 \ll E_F$, $p_F l \gg 1$, where l is the mean free path) for the orders $W_{x,i}$ and $W_{y,i}$,

$$\log \frac{T_c}{T_c^d} = \psi\left(\frac{1}{2} + \frac{\Gamma_{x,y}}{2\pi T_c^d}\right) - \psi\left(\frac{1}{2}\right), \tag{5}$$

where $\Gamma_x = 4\Gamma$, $\Gamma_y = 2\Gamma$, with $\Gamma = \pi u^2 n \nu_0$, where n is the impurity concentration. One can see the suppression rates are smaller for the $W_{y,i}$ orders that have been identified above as subleading ($T_c^y < T_c^x$). The transitions will be completely suppressed for $\Gamma_{\rm cr}^x = \frac{\pi}{8e^\gamma} T_c^x$ and $\Gamma_{\rm cr}^y = \frac{\pi}{4e^\gamma} T_c^y$, for the $W_{x,i}$ and $W_{y,i}$ orders, respectively. Thus, if $T_c^y/T_c^x > 1/2$, there exists a range of impurity concentrations such that the (spin) current order can overcome the competing CDW or AFM order.

Quantum critical point and unconventional superconductivity. Above we pointed out the possibility of suppressing the particle-hole orders by doping (see also Fig. 1). With the situation being similar to the high-T_c superconductors [43,44], it is natural to ask whether the fluctuations of the suppressed order around the critical doping can induce superconductivity. The interfermion interaction due to the critical fluctuations of a particle-hole order can be described by an effective action

$$S_{\rm QCP} = -\frac{gT}{\mathcal{V}} \sum_{p,p',q} \chi(q) c^\dagger_{p+q} \hat{W} c_p c^\dagger_{p'-q} \hat{W} c_{p'}, \tag{6}$$

where $\hat{W}$ is a matrix in the band and spin space corresponding to the particle-hole order parameter and $q \equiv (\mathbf{q}, \omega_n)$. $\chi(q)$ has the Ornstein-Zernike form $[\omega_n^2/c^2 + (\mathbf{q} - \mathbf{Q})^2 + \xi^{-2}]^{-1}$, with ξ being the correlation length of the fluctuations. Assuming $Q \ll p_F$ and not too small ξ, we can restrict our consideration to momentum-independent order parameters $\Delta_{\alpha,\alpha'} = \sum_{\mathbf{p}} \hat{c}_{p,\alpha}\hat{c}_{-p,\alpha'}$. The condition for the interaction to be attractive is ${\rm Tr}[\Delta^\dagger \hat{W} \Delta \hat{W}^T] > 0$. Moreover, only intraband $\sim\sigma_{0,z}$ pairing results in a logarithmic enhancement at low temperatures. For CDW QCP $\hat{W} \sim \sigma_x$ and conventional singlet superconductivity $\Delta \sim \sigma_0 \otimes is_y$ is promoted. For AFM QCP, on the other hand, $\hat{W} \sim \sigma_x \otimes \vec{s}$ and the singlet channel $\Delta \sim \sigma_z \otimes is_y$ is attractive. This type of pairing corresponds to a full-gap superconductivity with a sign change between the electron and hole Fermi surfaces similar to the $s_\pm$ state in the iron-based superconductors [43].

Outlook and conclusion. Our results can be readily applied to a number of proposed physical realizations of nodal surfaces [11,17,18]. For systems with few small nodal surfaces, such as YH_3 proposed in Ref. [17], one can expect that the long-range part of the Coulomb repulsion is likely to be the dominant interaction. On the other hand, in the case of graphene networks [11] one has two Dirac nodal surfaces ($N_0 = 4$) and thus the instability is likely to be driven by short-range repulsion or electron-phonon interactions not considered here. Finally, we note that the layered material ZrSiS is a promising candidate for hosting weakly dispersive nodal surfaces, with dispersion provided by the interlayer hopping. Recently, it has been studied in Ref. [45] using a 2D square lattice model with a nodal line.

Overall, our results show that systems with nodal surfaces could serve as a potential platform for realizing a multitude of quantum orders (Figs. 2 and 3) with many experimentally accessible "knobs," such as doping or disorder, to probe the phase diagram.

Acknowledgments. We acknowledge useful discussions with Tomáš Bzdušek. The work of S.M. is supported by the Emmy Noether Programme of German Research Foundation (DFG) under Grant No. MO 3013/1-1. P.A.V. acknowledges the support by the Rutgers University Center for Materials Theory Postdoctoral fellowhsip.

[1] A. M. Turner and A. Vishwanath, arXiv:1301.0330.
[2] A. Burkov, J. Phys.: Condens. Matter **27**, 113201 (2015).
[3] N. P. Armitage, E. J. Mele, and A. Vishwanath, Rev. Mod. Phys. **90**, 015001 (2018).
[4] S.-Y. Xu, I. Belopolski, N. Alidoust, M. Neupane, G. Bian, C. Zhang, R. Sankar, G. Chang, Z. Yuan, C.-C. Lee *et al.*, Science **349**, 613 (2015).
[5] B. Q. Lv, H. M. Weng, B. B. Fu, X. P. Wang, H. Miao, J. Ma, P. Richard, X. C. Huang, L. X. Zhao, G. F. Chen, Z. Fang, X. Dai, T. Qian, and H. Ding, Phys. Rev. X **5**, 031013 (2015).
[6] T. T. Heikkilä and G. E. Volovik, JETP Lett. **93**, 59 (2011).
[7] T. T. Heikkilä, N. B. Kopnin, and G. E. Volovik, JETP Lett. **94**, 233 (2011).
[8] A. A. Burkov, M. D. Hook, and L. Balents, Phys. Rev. B **84**, 235126 (2011).
[9] Y. Kim, B. J. Wieder, C. L. Kane, and A. M. Rappe, Phys. Rev. Lett. **115**, 036806 (2015).
[10] Q.-F. Liang, J. Zhou, R. Yu, Z. Wang, and H. Weng, Phys. Rev. B **93**, 085427 (2016).
[11] C. Zhong, Y. Chen, Y. Xie, S. A. Yang, M. L. Cohen, and S. Zhang, Nanoscale **8**, 7232 (2016).
[12] D. F. Agterberg, P. M. R. Brydon, and C. Timm, Phys. Rev. Lett. **118**, 127001 (2017).
[13] C. Timm, A. P. Schnyder, D. F. Agterberg, and P. M. R. Brydon, Phys. Rev. B **96**, 094526 (2017).
[14] T. Bzdušek and M. Sigrist, Phys. Rev. B **96**, 155105 (2017).
[15] O. Türker and S. Moroz, Phys. Rev. B **97**, 075120 (2018).
[16] M. Xiao and S. Fan, arXiv:1709.02363.
[17] J. Wang, Y. Liu, K.-H. Jin, X. Sui, L. Zhang, W. Duan, F. Liu, and B. Huang, Phys. Rev. B **98**, 201112(R) (2018).
[18] W. Wu, Y. Liu, S. Li, C. Zhong, Z.-M. Yu, X.-L. Sheng, Y. X. Zhao, and S. A. Yang, Phys. Rev. B **97**, 115125 (2018).
[19] Z. Wang and S.-C. Zhang, Phys. Rev. B **87**, 161107 (2013).
[20] J. Maciejko and R. Nandkishore, Phys. Rev. B **90**, 035126 (2014).
[21] B. Roy, P. Goswami, and V. Juričić, Phys. Rev. B **95**, 201102 (2017).
[22] S. Sur and R. Nandkishore, New J. Phys. **18**, 115006 (2016).

[23] P. Hosur, S. A. Parameswaran, and A. Vishwanath, Phys. Rev. Lett. **108**, 046602 (2012).
[24] H. Isobe and N. Nagaosa, Phys. Rev. B **86**, 165127 (2012).
[25] Y. Huh, E.-G. Moon, and Y. B. Kim, Phys. Rev. B **93**, 035138 (2016).
[26] A. A. Zyuzin and A. A. Burkov, Phys. Rev. B **86**, 115133 (2012).
[27] Y. Wang and P. Ye, Phys. Rev. B **94**, 075115 (2016).
[28] R. Nandkishore, Phys. Rev. B **93**, 020506 (2016).
[29] L. V. Keldysh and Y. Kopaev, Sov. Phys. Solid State **6**, 2219 (1965).
[30] P. Fulde and R. A. Ferrell, Phys. Rev. **135**, A550 (1964).
[31] A. I. Larkin and Y. N. Ovchinnikov, Sov. Phys. JETP **20**, 762769 (1965).
[32] J. Ye, Phys. Rev. B **60**, 8290 (1999).
[33] M. Y. Kharitonov and K. B. Efetov, Phys. Rev. B **78**, 241401 (2008).
[34] For the analysis presented in this Rapid Communication, relevant transfer momenta are of an order of p_F, while the condition of small momenta reads $q \ll q_{\mathrm{TF}} = \sqrt{4\pi e^2 \nu}$. As $\nu \sim N_0 p_F$, it is true either for a small p_F or for $N_0 \gg 1$. Additionally, we assume a weak-coupling limit, such that in the logarithmic approximation it is sufficient to consider only static ($\omega_n = 0$) screening [46].
[35] See Supplemental Material at http://link.aps.org/supplemental/10.1103/PhysRevB.98.241107 for details on modifications of the gap equation induced by $\delta(\theta, \varphi)$ and $\gamma(\theta, \varphi)$, the Hubbard-Stratonovich transformation for generic interactions, and effects of disorder on particle-hole instabilities.
[36] F. Chevy and C. Mora, Rep. Prog. Phys. **73**, 112401 (2010).
[37] T. M. Rice, Phys. Rev. B **2**, 3619 (1970).
[38] V. Cvetkovic and Z. Tesanovic, Phys. Rev. B **80**, 024512 (2009).
[39] A. B. Vorontsov, M. G. Vavilov, and A. V. Chubukov, Phys. Rev. B **79**, 060508 (2009).
[40] P. A. Lee and T. V. Ramakrishnan, Rev. Mod. Phys. **57**, 287 (1985).
[41] S. V. Syzranov and L. Radzihovsky, Annu. Rev. Condens. Matter Phys. **9**, 35 (2018).
[42] A. A. Abrikosov, L. P. Gorkov, and I. E. Dzyaloshinski, *Quantum Field Theoretical Methods in Statistical Physics* (Pergamon, Oxford, UK, 1965).
[43] P. J. Hirschfeld, M. M. Korshunov, and I. I. Mazin, Rep. Prog. Phys. **74**, 124508 (2011).
[44] D. J. Scalapino, Rev. Mod. Phys. **84**, 1383 (2012).
[45] A. N. Rudenko, E. A. Stepanov, A. I. Lichtenstein, and M. I. Katsnelson, Phys. Rev. Lett. **120**, 216401 (2018).
[46] M. Y. Kharitonov and K. B. Efetov, Semicond. Sci. Technol. **25**, 034004 (2010).